Compartmentalization established by claudin-11-based tight junctions in stria vascularis is required for hearing through generation of endocochlear potential

Shin-ichiro Kitajiri[1,2,3,*], **Tatsuo Miyamoto**[1,*], **Akihito Mineharu**[4], **Noriyuki Sonoda**[1], **Kyoko Furuse**[5], **Masaki Hata**[5], **Hiroyuki Sasaki**[5,6], **Yoshiaki Mori**[4], **Takahiro Kubota**[4], **Juichi Ito**[3], **Mikio Furuse**[1] **and Shoichiro Tsukita**[1,2,‡]

[1]Department of Cell Biology, Faculty of Medicine, Kyoto University, Sakyo-ku, Kyoto 606-8501, Japan
[2]Solution Oriented Research for Science and Technology, Japan Science and Technology Corporation, Sakyo-ku, Kyoto 606-8501, Japan
[3]Department of Otolaryngology Head and Neck Surgery, Faculty of Medicine, Kyoto University, Sakyo-ku, Kyoto 606-8507, Japan
[4]Department of Physiology II, Osaka Medical College, 2-7 Daigaku-machi, Takatsuki, 569-8686 Japan
[5]KAN Research Institute, Kyoto Research Park, Shimogyo-ku, Kyoto 606-8317, Japan
[6]Department of Molecular Cell Biology, Institute of DNA Medicine, The Jikei University School of Medicine, Nishi-Shinbashi, Minato-ku, Tokyo 105, Japan

*These authors contributed equally to this work
‡Author for correspondence (e-mail: htsukita@mfour.med.kyoto-u.ac.jp)

Summary

Claudins are cell adhesion molecules working at tight junctions (TJs) that are directly involved in compartmentalization in multicellular organisms. The cochlea includes a rather peculiar compartment filled with endolymph. This compartment is characterized by high K^+ concentration (~150 mM) and a positive endocochlear potential (~90 mV; EP), both indispensable conditions for cochlear hair cells to transduce acoustic stimuli to electrical signals. These conditions are thought to be generated by the stria vascularis, which is adjacent to the endolymph compartment. The stria vascularis itself constitutes an isolated compartment delineated by two epithelial barriers, marginal and basal cell layers. Because TJs of basal cells are primarily composed of claudin-11, claudin-11-deficient (Cld11$^{-/-}$) mice were generated with an expectation that the compartmentalization in stria vascularis in these mice would be affected. Auditory brainstem response measurements revealed that Cld11$^{-/-}$ mice suffered from deafness; although no obvious gross morphological malformations were detected in Cld11$^{-/-}$ cochlea, freeze-fracture replica electron microscopy showed that TJs disappeared from basal cells of the stria vascularis. In good agreement with this, tracer experiments showed that the basal cell barrier was destroyed without affecting the marginal cell barrier. Importantly, in the endolymph compartment of Cld11$^{-/-}$ cochlea, the K^+ concentration was maintained around the normal level (~150 mM), whereas the EP was suppressed down to ~30 mV. These findings indicated that the establishment of the stria vascularis compartment, especially the basal cell barrier, is indispensable for hearing ability through the generation/maintenance of EP but not of a high K^+ concentration in the endolymph.

Key words: Claudin, Compartmentalization, Tight junction, Cochlea, Stria vascularis

Introduction

In multicellular organisms, the internal environment must be isolated and buffered against the external environment, and further divided into various compositionally distinct fluid compartments. This compartmentalization is established by cellular sheets of epithelium delineating the body surface and cavities. Epithelial cellular sheets function as diffusion barriers and are also involved in active transport of materials across the barrier to dynamically maintain the internal environment of each compartment. For cellular sheets to exert these physiological functions, there must be some seal to the diffusion of solutes through the paracellular pathway. Tight junctions (TJs) have been shown to be responsible for this intercellular sealing in vertebrates (for reviews, see Schneeberger and Lynch, 1992; Anderson et al., 1995; Balda and Matter, 1998; Tsukita et al., 2001).

On ultrathin section electron microscopy, TJs appear as a series of discrete sites of apparent fusion, involving the outer leaflet of the plasma membranes of adjacent cells (Farquhar and Palade, 1963). On freeze-fracture electron microscopy, TJs appear as a set of continuous, anastomosing intramembranous particle strands (TJ strands) (for a review, see Staehelin, 1974). Our understanding of the molecular architecture of TJs has been rapidly unraveling in recent years. Three closely related proteins called ZO-1, ZO-2 and ZO-3 were identified as constituting the plaque structures underlying plasma membranes together with various other proteins (for a review, see Mitic and Anderson, 1998; González-Mariscal et al., 2000). TJ strands themselves were recently shown to be mainly composed of linearly polymerized integral membrane proteins called claudins with molecular masses of around 23 kDa (Furuse et al., 1998) (for reviews, see Tsukita and Furuse,

1999; Tsukita et al., 2001). Claudin molecules bear four transmembrane domains with both N- and C-termini located in the cytoplasm. Claudins compose a multigene family consisting of 24 members in human and mouse (Morita et al., 1999a) (for a review, see Tsukita et al., 2001). The expression pattern of claudins varies considerably among tissues. Most cell types express more than two claudin species in various combinations to constitute TJ strands. Within individual single strands, distinct species of claudins are co-polymerized to constitute 'heteropolymers' (Furuse et al., 1999). In addition to claudins, two other types of integral membrane proteins have been reported to concentrate at TJs, occludin (Furuse et al., 1993) and JAM (Martin-Padura et al., 1998).

As a focus for a discussion of how individual claudin species are involved in compartmentalization in multicellular organisms, the cochlea provides an advantageous experimental system (for a review, see Wangemann and Schacht, 1996). The cochlea includes two compositionally distinct fluid compartments, the scala vestibuli/tympani and the scala media, which are filled with perilymph and endolymph, respectively (reviewed in Ferrary and Sterkers, 1998; Wangemann, 2002) (Fig. 7A). These fluids are amazingly different in their chemical composition: Perilymph resembles extracellular fluids in general (for reviews, see Wangemann and Schacht, 1996; Ferrary and Sterkers, 1998), but endolymph has the characteristics of an intracellular fluid in that it has high K^+ and low Na^+ concentrations (for a review, see Sterkers et al., 1988). Furthermore, the electrical potential of endolymph [endocochlear potential (EP)] is positive by ~80-90 mV relative to perilymph (Tasaki and Spyropoulos, 1959; Konishi et al., 1978). It is now widely accepted that these characteristics of endolymph (high K^+ concentration and EP) are indispensable for cochlear hair cells to transduce acoustic stimuli into electrical signals (for a review, see Hudspeth, 1989). To maintain these characteristic features of endolymph, TJs are well developed in the epithelial cellular sheets delineating the endolymph compartment (the scala media) (Janke, 1975a; Janke, 1975b; Gulley and Reese, 1976). In good agreement, it has been reported that loss-of-function mutations of claudin-14, which are highly expressed in the organ of Corti of cochlea, caused hereditary deafness in humans (Wilcox et al., 2001).

Thus, the question is how the endolymph compartment with its peculiar chemical compositions and electrical potential is generated and maintained within the cochlea. The stria vascularis is thought to secrete K^+ from perilymph into endolymph and to generate an EP of +80-90 mV (von Bekesy, 1950; Tasaki and Spyroupoulos, 1959; Konishi et al., 1978; Wangemann et al., 1995; Wangemann, 2002). The stria vascularis is a highly vascularized epithelium and part of the epithelial cellular sheet delineating the endolymph compartment. Interestingly, it consists of two epithelial barriers carrying well-developed TJs – the marginal and basal cell layers (Janke, 1975a; Janke, 1975b) (Fig. 1B). This compartmentalization within the stria vascularis was hypothesized to be essentially important for the K^+ secretion and the EP generation (for a review, see Wangemann, 2002) but it was difficult to evaluate this hypothesis experimentally. In an earlier study, we found that claudin-11 was primarily expressed in TJs of basal cells in the stria vascularis (Kitajiri et al., 2004). Claudin-11 was previously reported to be expressed in large amounts in the oligodendrocytes in the brain and Sertoli cells in the testis (Morita et al., 1999b; Gow et al., 1999) but, in the inner ear, its expression was restricted to the basal cells. Therefore, in this study, with an expectation that the deficiency of claudin-11 selectively affects compartmentalization in the stria vascularis, we generated claudin-11-deficient mice and examined the cochlea of these mice in detail.

Materials and Methods
Antibodies
Rat anti-mouse occludin monoclonal antibody (mAb) (MOC37) and rabbit anti-mouse claudin-11 polyclonal antibody (pAb) were raised and characterized as described previously (Saitou et al., 1997; Morita et al., 1999b). Rabbit anti-human ZO-1 pAb was purchased from Zymed (San Francisco, CA). Anti-mouse ZO-1 mAb was produced in rats using the synthesized polypeptides corresponding to the N-terminal half of ZO-1 as an antigen. Rat anti-E-cadherin mAb (ECCD-2) was provided by M. Takeichi (RIKEN Center for Developmental Biology, Kobe, Japan).

Generation of claudin-11-deficient mice
The targeting vector was constructed by ligating a 6.0 kb *Hin*dIII/*Sma*I fragment and a 2.8 kb *Kpn*I/*Sca*I fragment, which are located upstream and downstream of exon 1, respectively, to the pgk-neo cassette. The diphtheria toxin A expression cassette (MC1pDT-A) was placed outside the 3′ arm of homology for negative selection. This targeting vector was designed to delete exon 1 (Fig. 2A), like the previous report of generation of claudin-11-deficient mice (Gow et al., 1999). J1 embryonic stem (ES) cells were electroporated with the targeting vector and selected for ~9 days in the presence of G418. G418-resistant colonies were removed and screened by Southern blotting with the 3′ external probe (Fig. 2B). Correctly targeted ES clones were identified by an additional 3.8-kb band together with the 5.8-kb band of the wild-type allele when digested with *Eco*RI. The targeted ES cells obtained were injected into C57BL/6 blastocysts, which were in turn transferred into Balb/c foster mothers to obtain chimeric mice. Male chimeras were mated with C57BL/6 females, and agouti offspring were genotyped to confirm the germ-line transmission of the targeted allele. The littermates were genotyped by Southern blotting. Heterozygous mice were then interbred to produce homozygous mice.

Auditory-brainstem-response measurements
Auditory-brainstem-response (ABR) measurements were performed in a soundproof room according to the method described previously (Zheng et al., 1999). In general, ABR waveforms were recorded for 12.8 milliseconds at a sampling rate of 40,000 Hz using 50-5000 Hz filter settings; waveforms recorded from 1024 stimuli at a frequency of 9 Hz were averaged. ABR waveforms were recorded in decreasing 5-dB sound pressure level (SPL) intervals from the maximum amplitude until no waveforms could be visualized.

Immunofluorescence microscopy
Temporal bones were removed from 10-week-old mice and the round and oval windows were opened, together with the small holes in the cochlear apical turn and superior semicircular canal. The perilymphatic space was gently perfused with 10% trichloroacetic acid (TCA) from the round to the oval window (Hayashi et al., 1999). Then the samples were immersed in 10% TCA for 1 hour, washed three times with PBS and decalcified with 5% EDTA in PBS for 3 days. Specimens were immersed in 30% sucrose in PBS for 1 day and

then frozen in liquid nitrogen. Frozen sections ~10 μm thick were cut from these samples and air dried on slide glasses. Frozen sections were treated with 0.2% Triton X-100 in PBS for 15 minutes, soaked in 1% bovine serum albumin in PBS and then incubated with primary antibodies for 30 minutes. They were then washed three times with PBS and incubated with secondary antibodies for 30 minutes. Cy3-conjugated anti-rat IgG pAbs or Alexa-488-conjugated anti-rabbit IgG pAbs were used as secondary antibodies. After being washed with PBS, samples were embedded in 95% glycerol in PBS containing 0.1% paraphenylendiamine and 1% *n*-propylgalate, and observed using a DeltaVision system (Version 2.10; Applied Precision) equipped with an Olympus IX70 microscope (Olympus, Tokyo, Japan) and a cooled charge-coupled device (CCD) system.

Freeze-fracture electron microscopy

Temporal bones obtained from 10-week-old mice were fixed by perilymphatic perfusion as described above with 2% glutaraldehyde in 0.1 M phosphate buffer (pH 7.2) overnight at 4°C and washed three times with 0.1 M phosphate buffer. The portion containing the stria vascularis was carefully dissected out, immersed in 30% glycerol in 0.1 M phosphate buffer for 2 hours and then frozen in liquid nitrogen. Frozen samples were fractured at –110°C and platinum shadowed unidirectionally at an angle of 45° in a Balzers Freeze Etching System (BAF060; Bal-Tec). Samples were then immersed in household bleach and replicas floating off the samples were washed with distilled water. Replicas were picked up on formvar-filmed grids and examined with an electron microscope (model H-7500; Hitachi).

Tracer permeability assay

Temporal bones were removed from 10-week-old mice and the round and oval windows were opened in PBS containing 1 mM $CaCl_2$. As mentioned above, the perilymph space was carefully perfused with 100 μl 10 mg ml^{-1} EZ-Link™ Sulfo-NHS-LC-Biotin (Pierce Chemical, Rockford, IL) in PBS containing 1 mM $CaCl_2$ for 5 minutes (Chen et al., 1997) followed by perfusion five times with PBS containing 1 mM $CaCl_2$. The temporal bones were then fixed by perilymphatic perfusion with 10% TCA for 1 hour and processed for immunofluorescence microscopy. The distribution of injected biotin tracer was visualized by incubating frozen sections with streptavidin/fluorescein-isothiocyanate (FITC) (Oncogene Research Products, Boston, MA) for 30 minutes.

Measurement of endocochlear potassium concentration and potential

10-week-old mice were anesthetized by an intraperitoneal and an intramuscular injection of the mixture of xylazine (12 mg kg^{-1}) and ketamine (50 mg kg^{-1}). The tympanic bulla was exposed using an opisthotic approach and double-barreled K^+-selective microelectrodes (or a pair of conventional and single-barreled K^+-selective microelectrodes) were inserted into the endolymph compartment (the scala media) of the basal turn under a stereomicroscope at 80-120× magnification (Model TS; Leitz, Germany). The single- and double-barreled K^+-selective microelectrodes were fabricated and evaluated as described previously (Fujimoto et al., 1988; Takamaki et al., 2003). The K^+-selective electrodes were filled with the K^+-selective liquid ion exchanger (Potassium Ionophore I – Cocktail B #60398; Fluka, Buchs, Switzerland). Each barrel of the microelectrodes for measurement of EP and the potassium potential was connected to a differential electrometer (FD-223; World Precision Instruments, FL) via an Ag/AgCl pellet (MEH1SF; World Precision Instruments), and the outputs of the endolymph were connected to a four-channel recorder (U-638, Nippon Denshi Kagaku, Tokyo, Japan) and a Mac Lab 8s (ADInstruments, New South Wales, Australia). The output of the electromotive force (EMF) from K^+-selective microelectrodes was

recorded by subtracting the EMF from the microelectrode measuring EP with a differential electrometer.

The potassium concentration in the endolymph ($[K]_e$) was calculated according to the following equation,

$$[K]_e = 150 \times 10^{(E150-EKe)\div\alpha},$$

where E150 is the voltage from the output of the K^+-selective microelectrode in a 150 mM KCl solution, EKe is the voltage difference between the endocochlear voltage K^+-selective microelectrode and endocochlear potentials (EP), and α is the slope constant of the K^+-selective microelectrodes. The recording in the endolymph was accepted only when the EP was stable for more than 30 seconds.

Results

Claudin-11 in stria vascularis of wild-type mice

On the lateral wall of the cochlear duct of wild-type mice, the stria vascularis was easily identified as a band of specialized stratified epithelium (Fig. 1A). As shown in Fig. 1B, the cochlear stria vascularis consists mainly of two epithelial cell layers, marginal and basal. Marginal cells, that face the endolymph compartment (the scala media) with their apical membranes are simple epithelia with well-developed TJs at the most apical portion of their lateral membranes and with a labyrinthine system of narrow cell process at their basal portion. Basal cells also have many cellular processes and establish another barrier by adhering to each other through well-developed TJs. These findings indicate that the stria vascularis itself constitutes an isolated compartment in the cochlea (intrastrial space; II in Fig. 1B).

In an earlier study, we examined the expression and distribution patterns of claudins in the mouse inner ear (Kitajiri et al., 2004): Marginal cells expressed numerous species of claudins such as claudins 1, 2, 3, 8, 9, 10, 12, 14 and 18, whereas only claudin-11 was detectable in basal cells. As shown in Fig. 1C, when frozen sections of stria vascularis were double stained with anti-claudin-11 pAb and anti-occludin mAb, occludin-positive TJs were observed both in marginal and basal cell layers, whereas claudin-11 was exclusively concentrated at TJs of basal cells. Thus, we expected that the deficiency of claudin-11 would selectively affect the barrier of basal cell layers.

Generation of claudin-11-deficient mice and their hearing ability

We produced mice unable to express claudin-11. Nucleotide sequencing as well as restriction mapping identified three exons that cover the whole open reading frame of *Cld11*. The putative exon 1 contained the first ATG and encoded the N-terminal portion (amino acids 1-75) of the claudin-11 molecule containing the first transmembrane domain and a part of the first extracellular loop (Fig. 2A). We constructed a targeting vector that was designed to disrupt the *Cld11* gene by replacing exon 1 with the neomycin resistance gene (Fig. 2A). Mice were generated from ES cell clones in which the *Cld11* gene was disrupted by homologous recombination. Southern blotting confirmed the disruption of the *Cld11* gene in heterozygous as well as homozygous mutant mice (Fig. 2B), and a reverse-transcription polymerase chain reaction
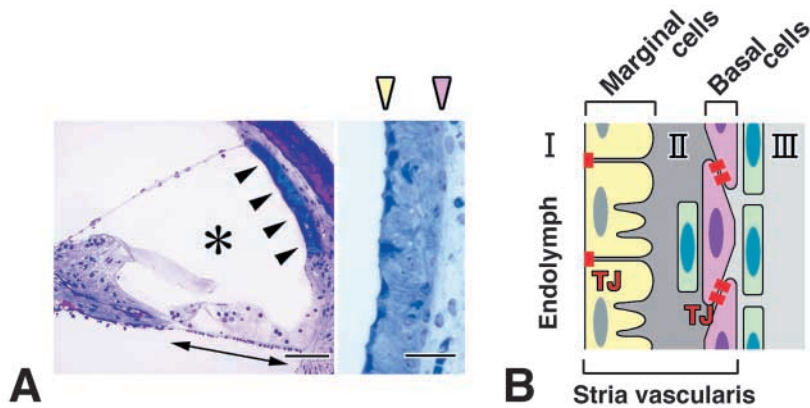
Fig. 1. Stria vascularis and claudin-11 in 10-week-old wild-type mice. (A) Toluidine-blue-stained Epon semi-thin sections of the wild-type cochlea. (left) Stria vascularis (arrowheads) are located on the lateral wall of the cochlear duct. Asterisk, scala media; arrow, the organ of Corti. (See also Fig. 7A.) (right) Stria vascularis is enlarged. Yellow and pink arrowheads represent the marginal and basal cell layers, respectively. (B) Schematic drawing of the cellular architecture of stria vascularis. Three compartments are represented: compartment I (I) is the scala media filled with endolymph; compartment II (II) is the intrastrial space delineated by marginal and basal cell layers; compartment III (III) is connective tissue of the spiral ligament connected to the perilymphatic space. Green cells in compartments II and III are called 'intermediate cells' and 'fibrocytes', respectively. (C) Double immunofluorescence microscopy of frozen sections of stria vascularis with anti-claudin-11 pAb and anti-occludin mAb (a) or anti-ZO-1 pAb and anti-E-cadherin mAb (b). Occludin is concentrated at TJs of both marginal (yellow arrowhead) and basal (pink arrowhead) cell layers, whereas claudin-11 is detected only in TJs of basal cell layers. In frozen sections, TJs of marginal cells appear as dots, but those of basal cells are observed as discontinuous short lines. ZO-1 and E-cadherin are concentrated at cell-cell borders of both layers but do not colocalize. Bars, 50 μm (A, left), 20 μm (A, right, C).
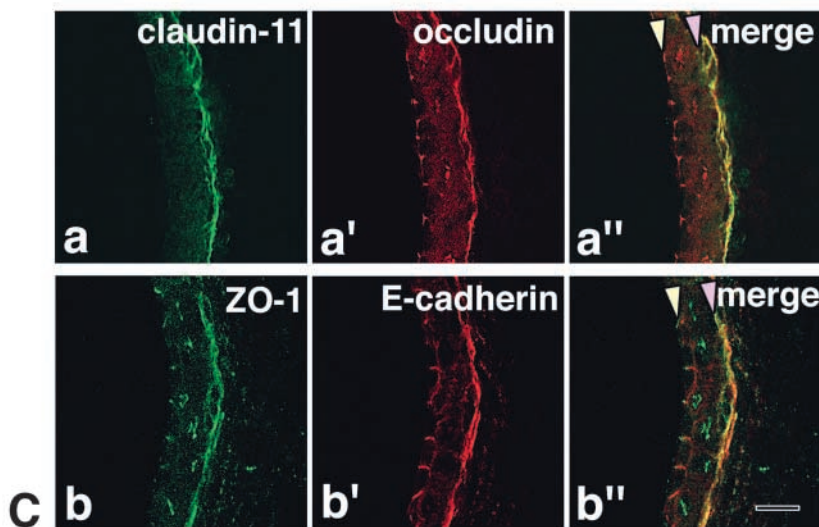
detected no *Cld11* mRNA from the testis of homozygous mutant mice (Fig. 2C).

Claudin-11-deficient (*Cld11*$^{-/-}$) mice were born in the expected Mendelian ratios and looked normal macroscopically. We had previously found that claudin-11 is mainly expressed in oligodendrocytes in the brain and Sertoli cells in the testis (Morita et al., 1999b); in good agreement with this, Gow et al.

(Gow et al., 1999) reported that mice lacking the expression of claudin-11 exhibited neurological and reproductive deficits (weakness of hindlimb and male sterility). Our newly generated *Cld11*$^{-/-}$ mice also showed these deficits (data not shown).

We then examined the hearing ability of *Cld11*$^{-/-}$ mice. The ABR was measured in 10-week-old *Cld11*$^{+/+}$ and *Cld11*$^{-/-}$ mice

Fig. 2. Generation of claudin-11-deficient mice. (A) Restriction maps of the wild-type allele, the targeting vector and the targeted allele of the mouse *Cld11* gene. The first ATG codon was located in the putative exon 1, which encoded the N-terminal portion (amino acids 1-75) of the claudin-11 molecule containing the first transmembrane domain and the first extracellular loop. The targeting vector contained a pgk neo cassette in its middle portion to delete exon 1 in the targeted allele. The position of the probe for Southern blotting is indicated as a bar. E, *Eco*RI; B, *Bgl*II. (B) Genotype analyses by Southern blotting of *Eco*RI-digested genomic DNA from wild-type (+/+), heterozygous (+/–) and homozygous (–/–) mice for the mutant *Cld11* allele. Southern blotting with the probe indicated in A yielded a 5.8-kb and a 3.8-kb band from the wild type and the targeted allele, respectively. (C) Loss of *Cld11* mRNA in the testis of claudin-11-defcient mice examined by reverse-transcription polymerase chain reaction. As a control, the hypoxanthine-phosphoribosyl-transferase-encoding gene (*HPRT*) was equally amplified in all samples.

in response to a stimuli with a sound pressure level (SPL) of 0-80 dB (16 kHz). As shown in Fig. 3A, hearing ability was significantly affected in $Cld11^{-/-}$ mice. The hearing thresholds of 10-week-old $Cld11^{+/+}$, $Cld11^{+/-}$ and $Cld11^{-/-}$ mice are summarized in Fig. 3B. $Cld11^{+/+}$ and $Cld11^{+/-}$ mice showed normal hearing thresholds (10-20 dB SPL), whereas $Cld11^{-/-}$ mice showed abnormally increased hearing thresholds (40-60 dB SPL).

TJs in stria vascularis of $Cld11^{-/-}$ mice

We compared light microscopic images of toluidine blue-stained sections prepared from Epon-embedded tissues of the inner ear between $Cld11^{+/+}$ and $Cld11^{-/-}$ mice aged 10 weeks, but no obvious gross morphological malformations were observed in $Cld11^{-/-}$ cochlea (Fig. 4A). On the lateral wall of the $Cld11^{-/-}$ cochlea, stria vascularis was easily identified normally except for some edematous appearance. We then examined the distribution of claudin-11, occludin, ZO-1 and E-cadherin in the $Cld11^{-/-}$ stria vascularis by immunofluorescence microscopy (Fig. 4B). TJs in marginal cell layers did not appear to be affected: both occludin and ZO-1 were concentrated at the most apical region of their lateral membranes. By contrast, in basal cell layers lacking expression of claudin-11, neither occludin nor ZO-1 was clearly concentrated at cell-cell adhesion sites, where E-cadherin was concentrated. These findings suggested that, in $Cld11^{-/-}$ stria

vascularis, TJs disappeared from basal cell layers, although the cellular organization of stria vascularis did not appear to be extensively affected. Indeed, this was confirmed by freeze-fracture replica electron microscopy. As previously reported (Janke, 1975a; Janke, 1975b), TJs of basal cells in $Cld11^{+/+}$ stria vascularis were characterized by many parallel strands that did not extensively anastomose (Fig. 5a). From low-power freeze-fracture replica images obtained from $Cld11^{-/-}$ stria vascularis, we successfully identified marginal and basal cell layers (Fig. 5b). Marginal cells bore well-developed TJs (Fig. 5c), whereas no TJ strands were observed between adjoining basal cells (Fig. 5d).

Functional alterations of $Cld11^{-/-}$ stria vascularis

The question then arose of whether the barrier of basal cell layers of stria vascularis is affected in $Cld11^{-/-}$ mice, and so
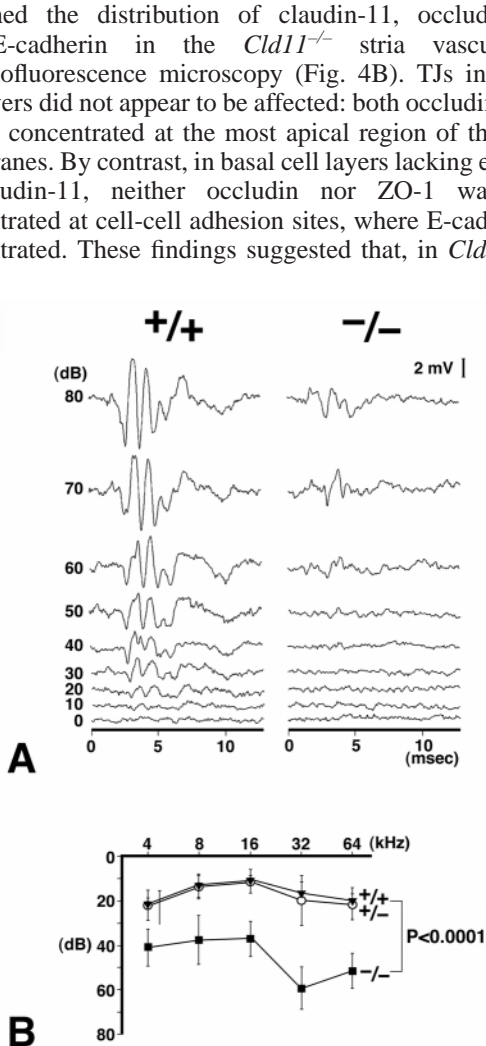
Fig. 4. Stria vascularis in 10-week-old $Cld11^{-/-}$ mice. (A) Toluidine-blue-stained Epon semi-thin sections of the cochlea of $Cld11^{-/-}$ mice. (left) Stria vascularis (arrowheads) are located on the lateral wall of the cochlear duct and there are no obvious gross morphological malformations compared with the $Cld11^{+/+}$ cochlea (Fig. 1A). Asterisk, scala media; arrow, the organ of Corti. (See also Fig. 7A.) (right) The stria vascularis is enlarged. Yellow and pink arrowheads represent the marginal and basal cell layers, respectively. (B) Double immunofluorescence microscopy of frozen sections of $Cld11^{-/-}$ stria vascularis with anti-claudin-11 pAb and anti-occludin mAb (a) or anti-ZO-1 mAb and anti-E-cadherin pAb (b). Claudin-11 completely disappears from TJs of basal cell layers (pink arrowhead) and signals of other TJ markers such as occludin and ZO-1 also appear to be decreased in basal cells. Occludin- and ZO-1-positive TJs are normally detected from marginal cell layers (yellow arrowhead). The E-cadherin staining pattern suggests that the cellular architecture is not extensively disorganized. Bars, 50 μm (A, left), 20 μm (A, right, B).

Fig. 3. Deafness in $Cld11^{-/-}$ mice. (A) ABR to stimuli of 0-80 dB sound pressure level (16 kHz) in 10-week-old $Cld11^{+/+}$ and $Cld11^{-/-}$ mice. (B) Hearing thresholds of 10-week-old $Cld11^{+/+}$, $Cld11^{+/-}$ and $Cld11^{-/-}$ mice at various sound frequencies. $Cld11^{+/+}$ and $Cld11^{+/-}$ mice show normal hearing thresholds (10-20 dB SPL), whereas $Cld11^{-/-}$ mice show abnormally increased hearing thresholds (40-60 dB SPL).
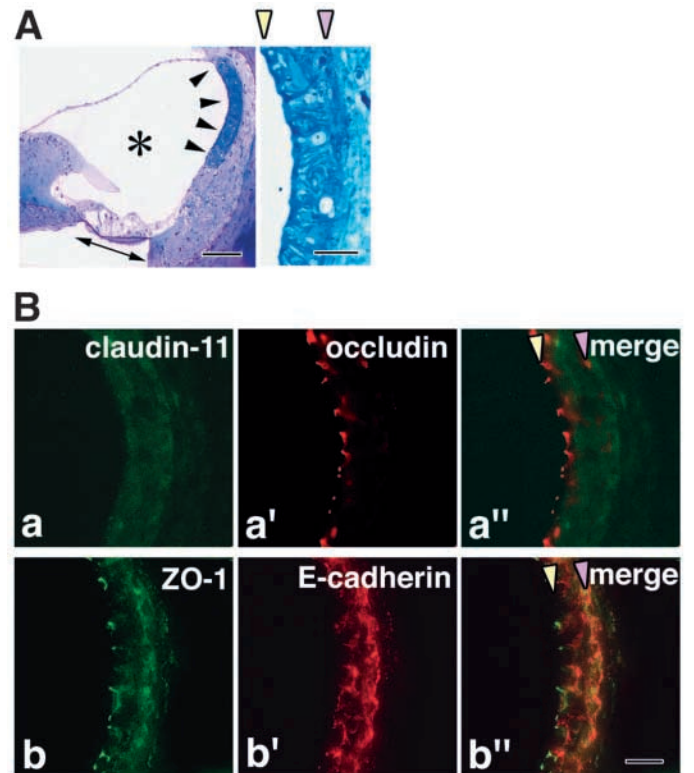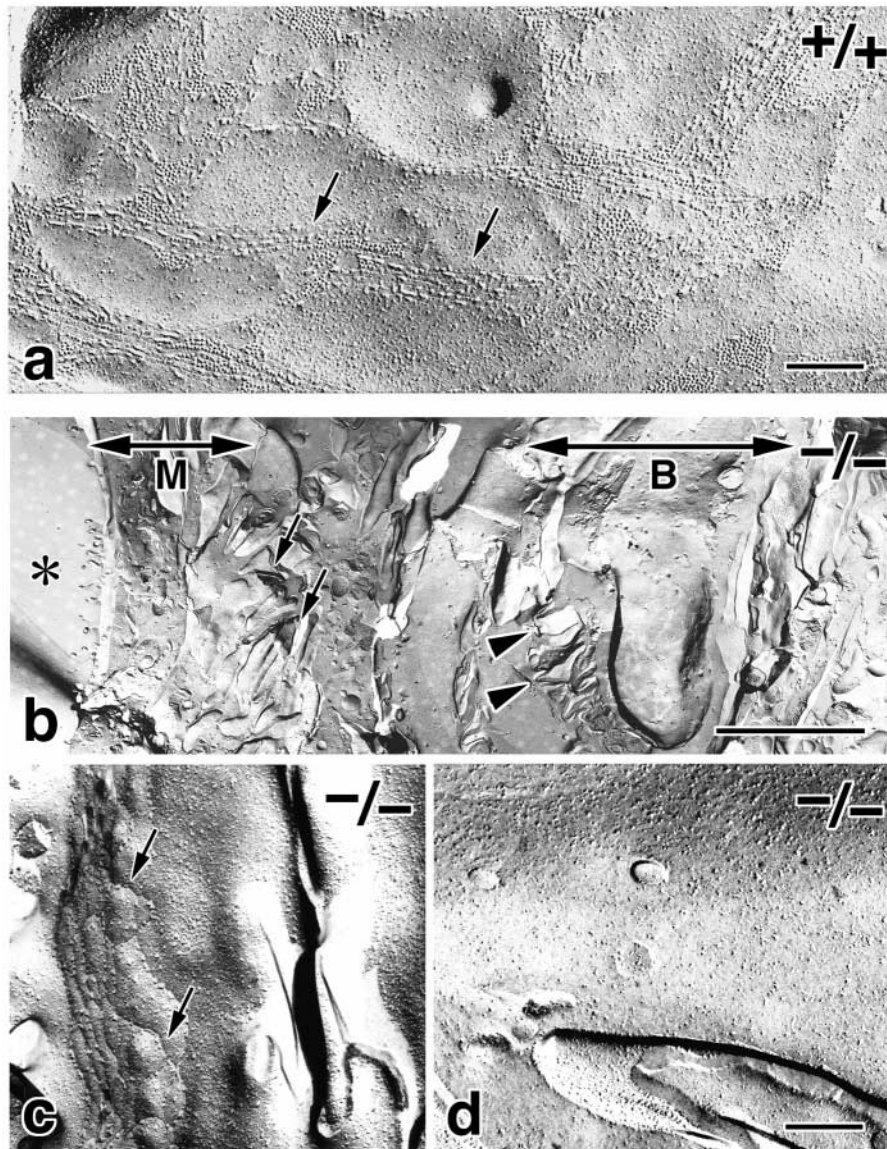
Fig. 5. Freeze-fracture replica electron microscopy. As previously reported (Janke, 1975a; Janke, 1975b; Gulley and Reese, 1976), TJs of basal cell layers of $Cld11^{+/+}$ stria vascularis are characterized by many parallel strands (arrows) that do not extensively anastomose (a). In a low-power replica image of $Cld11^{-/-}$ stria vascularis, marginal (M) and basal (B) cell layers can be identified (b). Arrows and arrowheads represent the basal cellular processes of marginal cells and cell-cell contact sites of basal cells, respectively. Asterisk, scala media. At the most apical region of the lateral membrane of marginal cells of $Cld11^{-/-}$ stria vascularis, TJ strands (arrows) are well developed continuously (c) but, at the cell-cell contact planes between adjacent basal cells on the same replica, no TJ strands are observed (d). Bars, 200 nm (a), 2 μm (b), 200 nm (c,d).

we performed a tracer experiment. Temporal bones were removed, and the round and oval windows were opened. Then, the perilymph compartment was gently perfused from the round to oval windows with an isotonic solution containing a primary amine-reactive biotinylation reagent (557 Da), which covalently cross-links to an accessible cell surface. After a 5 minute incubation followed by perfusion with PBS, the cochlea was dissected out, fixed and frozen. Frozen sections of stria vascularis were double labeled with anti-E-cadherin pAb (red) and streptavidin (green) to detect cell layers and bound biotin, respectively (Fig. 6). In $Cld11^{+/+}$ stria vascularis, the biotinylation reagent diffused freely through the connective tissue, represented as 'compartment III' in Fig. 1B, but did not get into the intrastrial space ('compartment II' in Fig. 1B). In sharp contrast to this, the diffusion of the biotinylation reagent in $Cld11^{-/-}$ cochlea was not stopped at the basal cell layers, but the reagent appeared to pass them to reach the intrastrial space of the stria vascularis. Interestingly, this reagent did not diffuse into the endolymph compartment across the marginal cell

layers ('compartment I' in Fig. 1B). These findings clearly indicated that, in stria vascularis, a deficiency of claudin-11 affects the barrier of basal cell layers but not of marginal cell layers.

Stria vascularis has long been believed to be the motor of K^+ secretion into endolymph and the origin of the endocochlear potential (EP) (for a review, see Wangemann, 2002). Therefore, we next compared K^+ concentrations of endolymph and EPs between $Cld11^{+/+}$ and $Cld11^{-/-}$ cochlea. For this purpose, a double-barreled K^+-selective microelectrode or a pair of single-barreled K^+-selective and conventional microelectrodes was directly inserted into the endolymph compartment (the scala media) of the basal turn of cochlea of $Cld11^{+/+}$ and $Cld11^{-/-}$ mice under anesthetic (Fig. 7A). Interestingly (Fig. 7B), the claudin-11 deficiency (i.e. the destruction of the barrier of basal cell layers) did not change the potassium concentration of the endolymph [$Cld11^{+/+}$, 148±7 mM (n=6); $Cld11^{-/-}$, 145±6 mM (n=6)] but significantly suppressed the generation of EP [$Cld11^{+/+}$, 95±6 mV (n=6); $Cld11^{-/-}$, 31±14 mV (n=6)].
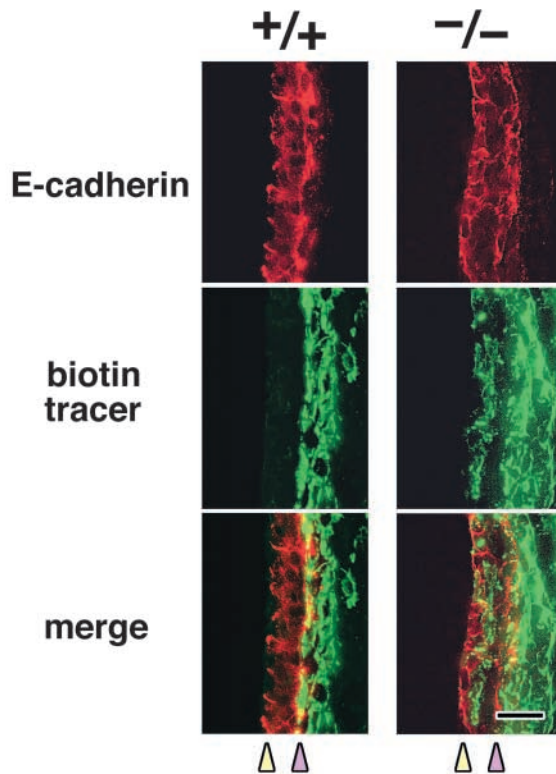
Fig. 6. Tracer-permeability assay of the stria vascularis of 10-week-old *Cld11*$^{+/+}$ and *Cld11*$^{-/-}$ mice. An isotonic solution containing freshly made biotinylation reagent was injected into the perilymph space from the round window of the cochlea and, after a 5 minute incubation followed by washing with PBS, the cochlea was dissected out, fixed and frozen. Frozen sections were double stained with anti-E-cadherin pAb (red) and streptavidin (green) to detect cell layers and bound biotin, respectively. In the *Cld11*$^{+/+}$ stria vascularis, the biotinylation reagent diffused freely through the connective tissue, represented as 'compartment III' in Fig. 1B, but did not get into the intrastrial space ('compartment II' in Fig. 1B). In sharp contrast to this, in the *Cld11*$^{-/-}$ cochlea, diffusion of the biotinylation reagent was not stopped at the basal cell layers but the reagent appeared to pass through them to reach the intrastrial space. Yellow and pink arrowheads represent the marginal and basal cell layers, respectively. Bar, 20 μm.

Discussion

For homeostasis in multicellular organisms, various compositionally distinct fluid compartments must be established through the barrier function of TJs in epithelial and endothelial cells. Recent identification of claudins, cell adhesion molecules responsible for the TJ barrier, opened a new way to perturb individual compartments and to evaluate the physiological relevance of each compartment at a whole-body level. To date, 24 members of the claudin family have been identified in humans and mice, and these are reported to be expressed in individual cell layers in various combinations and mixing ratios (for reviews, see Tsukita et al., 2001; Gonzalez-Mariscal et al., 2003). It has been shown that a particular compartment can be destroyed when the gene for major species of claudins constituting TJs of its delineating epithelial cell layer is homozygously knocked out in mice. For example, claudin-1 was expressed in large amounts in the epidermis and claudin-1-deficient mice showed severe dysfunction of the epidermal barrier, being dehydrated quickly after birth (Furuse et al., 2002). Endothelial cells of brain blood vessels primarily expressed claudin-5 and, in claudin-5-deficient mice, the blood-brain barrier was severely affected (Nitta et al., 2003). The *Cld11* gene, which this study focused on, has already been knocked out by Gow et al. (Gow et al., 1999) and, in these mice, the compartments established by oligodendrocyte myelin sheaths and Sertoli cells were affected, resulting in neurological and reproductive deficits.

From the viewpoint of compartmentalization, the cochlea is most intriguing. In particular, endolymph is unique in its high K$^+$ concentration and positive electrical potential, the EP (for a review, see Ferrary and Sterkers, 1998). Accumulated evidence indicates that the stria vascularis is the actual site where K$^+$ is secreted into endolymph and the EP is generated (for reviews, see Wangemann et al., 1995; Wangemann, 2002). Interestingly, the stria vascularis itself constitutes a tube-like isolated fluid compartment delineated by two distinct, marginal and basal, cell layers. This tubular compartment runs spirally in tight association with the endolymph compartment, the scala media. The question thus naturally arose about stria vascularis of what, in terms of its K$^+$ secretion and the EP generation, is the physiological relevance of the establishment of such a peculiar compartment. One of the most conclusive ways to answer this was selectively to destroy the stria vascularis compartment and to examine the effects on hearing ability itself and the K$^+$ concentration and EP of the endolymph. We previously examined the expression patterns of claudins in the cochlea in detail, and found that claudin-11 was the major constituent of TJs of basal cell layers of stria vascularis (Kitajiri et al., 2004). In good agreement with this, TJs of these cells were reported to be characterized by parallel, densely packed strands (Janke, 1975a; Janke, 1975b; Gulley and Reese, 1976), which were also observed in claudin-11-based TJs of Sertoli cells (Gilula et al., 1976; Russell et al., 1985). Considering that the claudin-11 expression was restricted to the basal cell layers of stria vascularis, these findings led us to speculate that, when the *Cld11* gene is knocked out, the stria vascularis compartment is selectively destroyed without affecting other cochlear compartments. We thought that this speculation could be evaluated experimentally, because claudin-11-deficient mice were reported to be born alive and grow without severe defects (Gow et al., 1999).

Then, we generated claudin-11-deficient (*Cld11*$^{-/-}$) mice using a conventional homologous recombination method and examined the structure and functions of their cochlea, especially of stria vascularis, in detail. ABR measurements showed that *Cld11*$^{-/-}$ mice suffered from deafness. As expected, in *Cld11*$^{-/-}$ cochlea no obvious gross morphological malformations were observed and the tracer experiments clearly revealed that the barrier function of basal cell layers, but not marginal cell layers, of stria vascularis was severely affected. Very interestingly, when the K$^+$ concentration and EP were measured directly using K$^+$-sensitive microelectrodes from the scala media, in *Cld11*$^{-/-}$ cochlea, the K$^+$ concentration was maintained around a normal level (~150 mM) but the latter was significantly suppressed down to ~30 mV. These findings led to two conclusions. The first, that the barrier function of the marginal cell layer is sufficient for generation and maintenance of the high K$^+$ concentration of endolymph. This

is consistent with previous electrophysiological data (Konishi et al., 1978; Wangemann et al., 1995). The second conclusion is that the basal cell barrier [i.e. the compartmentalization in stria vascularis (intrastrial space)] is indispensable for the generation and maintenance of the EP.

As regards the mechanisms for generation of EP, two distinct models have been proposed, a 'single-cell model' and a 'two-cell model' (Fig. 8) (for a review, see Wangemann, 1995). The single-cell model hypothesizes that Na^+ conductance of the basolateral membrane of marginal cells generates a large positive membrane voltage that is the source for the positive EP (Offner et al., 1987). In this model, the contribution of basal cell layers to the EP generation is not considered. In the two-cell model, K^+ conductance localized to the inner membrane of basal cells and to intermediate cells that are connected to basal cells through gap junctions, which were assumed to generate the source of EP (Salt et al., 1987; Kikuchi et al., 1995). In this model, the involvement of marginal cells in the generation of EP was limited to the maintenance of the low K^+ concentration in the intrastrial space. Recent detailed electrophysiological data appear to favor the two-cell model (Wangemann et al., 1995; Takeuchi et al., 1995; Takeuchi et al., 2000; Marcus et al., 2002), but it was technically difficult to evaluate conclusively the importance of the compartmentalization in the stria vascularis for the EP generation.

Set against this situation, the data obtained in this study clearly supported the two-cell model (Fig. 8). It is difficult to explain the downregulation of EP in $Cld11^{-/-}$ cochlea by the one-cell model. Interestingly, the EP in $Cld11^{-/-}$ cochlea was not suppressed completely down to 0 mV, but still showed ~30 mV. It is likely that this voltage simply represents a residual electrical resistance between the intrastrial space and the spiral ligament, because that space is extremely small and tortuous in shape. $Cld11^{-/-}$ mice would be useful in future experiments aiming to evaluate this speculation.

Claudin-11 was shown to constitute TJ strands between lamellae of myelin sheaths of oligodendrocytes in the brain, and between adjacent Sertoli cells in the testis (Morita et al., 1999b). In claudin-11-deficient mice, as established by Gow et al. (Gow et al., 1999), TJ strands were absent in myelin sheaths of oligodendrocytes and Sertoli cells, conclusively demonstrating that, in these types of cell, TJ strands are mainly composed of a single specific claudin, claudin-11. In this study, we established another line of $Cld11^{-/-}$ mice and demonstrated that TJ strands in basal cells of stria vascularis in the cochlea were also singly composed of claudin-11. This situation is peculiar, because in most epithelial cellular sheets, TJ strands are composed of more than two distinct species of claudins as heteropolymers (for a review, see Tsukita et al., 2001). Interestingly, in addition to oligodendrocytes, Sertoli cells and
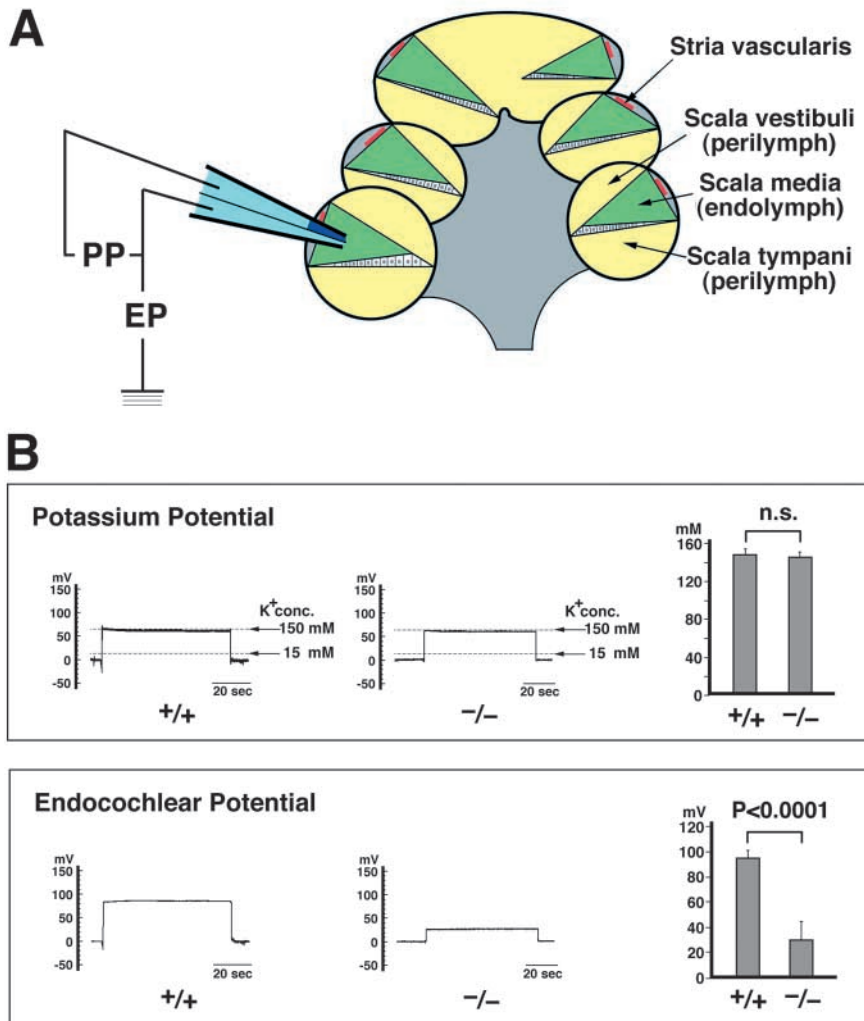

Fig. 7. Potassium concentration and endocochlear potential (EP) of endolymph. (A) The method for recording the potassium potential (PP) and EP. A double-barreled K^+-selective microelectrode is directly inserted into the scala media of the basal turn of the cochlea of 10-week-old mice under anesthetic. (B) Recordings of PP and EP of endolymph in $Cld11^{+/+}$ and $Cld11^{-/-}$ cochlea. $Cld11^{+/+}$ and $Cld11^{-/-}$ cochlea showed similar PPs (~70 mV), indicating that endolymph of both $Cld11^{+/+}$ and $Cld11^{-/-}$ cochlea contained similar K^+ concentrations [$Cld11^{+/+}$, 148±7 mM ($n=6$); $Cld11^{-/-}$, 145±6 mM ($n=6$)]. By contrast, the EP of $Cld11^{-/-}$ cochlea [31±14 mV ($n=6$)] is significantly lower than that of $Cld11^{+/+}$ cochlea [95±6 mV ($n=6$)].
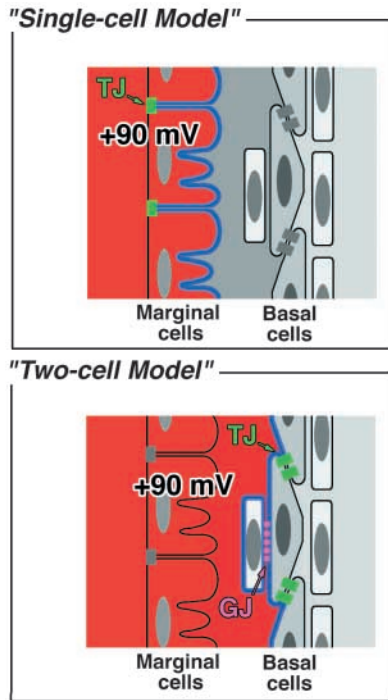
Fig. 8. Two models for the mechanism behind generation of EP. The 'single-cell model' hypothesizes that the Na^+ conductance of the basolateral membranes of marginal cells (blue lines) generates a large positive membrane voltage, which is the source for the positive EP (~90 mV; red zone). In this model, TJs in marginal cells (green) are thought to be essential for EP generation. In the 'two-cell model', the K^+ conductance in the inner membranes (blue lines) of basal cells and of intermediate cells, which are connected to basal cells through gap junctions (GJ), are assumed to generate the source of EP (~90 mV; red zone). In this model, the involvement of marginal cells in the generation of EP was limited to the maintenance of the low K^+ concentration in the intrastrial space and TJs in basal cells (green) play a crucial role.

cochlear basal cells, claudin-11 is reported to be expressed in renal epithelial cells of the thick ascending limb of Henle, in which, by contrast, claudin-11 appeared to form heteropolymers together with claudins 3, 10 and 16 (Kiuchi-Saishin et al., 2002). Through detailed analyses of claudin-11-deficient mice, we can now state that three important physiological processes, saltatory conduction along axons, spermatogenesis and hearing are fully dependent on the compartmentalization established by TJ strands consisting of a single species of claudin, claudin-11. A question then naturally arises: why is claudin-11 used singly for such important physiological processes, even though there are many other claudin species? It is still too soon to answer this question, but these findings indicate that the physiological relevance of the existence of many claudin species is not a simple safety measure based on functional redundancy. TJs are not a simple barrier: they show ion and size selectivity, and the tightness of their barrier function varies significantly depending on cell type. That cell-type-specific properties of TJ strands are determined by the combination and mixing ratios of claudins within individual TJ strands is widely accepted, so it is fascinating to speculate that TJs in oligodendrocytes, Sertoli

cells and cochlear basal cells are highly specialized in terms of their barrier function, which could be why claudin-11 is used singly in these TJs. $Cld11^{-/-}$ mice will provide a valuable resource in the future, not only for further study of the molecular mechanisms of hearing but also for gaining a better understanding of the physiological relevance of the existence of so many claudin species.

References

Anderson, J. M. and van Itallie, C. M. (1995). Tight junctions and the molecular basis for regulation of paracellular permeability. *Am. J. Physiol.* **269**, G467-G475.

Balda, M. S. and Matter, K. (1998). Tight junctions *J. Cell Sci.* **111**, 541-547.

Chen, Y.-H., Merzdorf, C., Paul, D. L. and Goodenough, D. A. (1997). COOH terminus of occludin is required for tight junction barrier function in early *Xenopus* embryos. *J. Cell Biol.* **138**, 891-899.

Farquhar, M. G. and Palade, G. E. (1965). Cell junctions in amphibian skin. *J. Cell Biol.* **26**, 263-291.

Ferrary, E. and Sterkers, O. (1998). Mechanisms of endolymph secretion. *Kidney Int.* **65**, S98-S103.

Fujimoto, M., Morimoto, Y. and Kubota, T. (1988). Dependence of cell pH and buffer capacity on the extracellular acid-base change in the skeletal muscle of bullfrog. *Jpn J. Physiol.* **38**, 799-818.

Furuse, M., Hirase, T., Itoh, M., Nagafuchi, A., Yonemura, S., Tsukita, S. and Tsukita, S. (1993). Occludin: a novel integral membrane protein localizing at tight junctions. *J. Cell Biol.* **123**, 1777-1788.

Furuse, M., Fujita, K., Hiiragi, T., Fujimoto, K. and Tsukita, S. (1998). Claudin-1 and -2: novel integral membrane proteins localizing at tight junctions with no sequence similarity to occludin. *J. Cell Biol.* **141**, 1539-1550.

Furuse, M., Sasaki, H. and Tsukita, S. (1999). Manner of interaction of heterogeneous claudin species within and between tight junction strands. *J. Cell Biol.* **14**, 891-903.

Furuse, M., Hata, M., Furuse, K., Yoshida, Y., Haratake, A., Sugitani, Y., Noda, T., Kubo, A. and Tsukita, S. (2002). Claudin-based tight junctions are crucial for the mammalian epidermal barrier: a lesson from claudin-1-deficient mice. *J. Cell Biol.* **156**, 1099-1111.

Gilula, N. B., Fawcett, D. W. and Aoki, A. (1976). The Sertoli cell occluding junctions and gap junctions in mature and developing mammalian testis. *Dev. Biol.* **50**, 142-168.

González-Mariscal, L., Betanzos, A. and Avila-Flores, A. (2000). MAGUK proteins: structure and role in the tight junction. *Semin. Cell Dev. Biol.* **11**, 315-324.

Gonzalez-Mariscal, L., Betanzos, A., Nava, P. and Jaramillo, B. E. (2003). Tight junction proteins. *Prog. Biophys. Mol. Biol.* **81**, 1-44.

Gow, A., Southwood, C. M., Li, J. S., Pariali, M., Riordan, G. P., Brodie, S. E., Danias, J., Bronstein, J. M., Kachar, B. and Lazzarini, R. A. (1999). CNS myelin and Sertoli cell tight junction strands are absent in OSP/claudin-11 null mice. *Cell* **99**, 649-659.

Gulley, R. L. and Reese, T. S. (1976). Intercellular junctions in the reticular lamina of the organ of Corti. *J. Neurocytol.* **5**, 479-507.

Hayashi, K., Yonemura, S., Matsui, T., Tsukita, S. and Tsukita, S. (1999). Immunofluorescence detection of ezrin/radixin/moesin (ERM) proteins with their carboxyl-terminal threonine phosphorylated in cultured cells and tissues: application of a novel fixation protocol using trichloroacetic acids (TCA) as a fixative. *J. Cell Sci.* **112**, 1149-1158.

Hudspeth, A. J. (1989). How the ear's works work. *Nature* **341**, 397-404.

Janke, K. (1975a). Intercellular junctions in the guinea pig stria vascularis as shown by freeze-etching. *Anat. Embryol.* **147**, 189-201.

Janke, K. (1975b). The fine structure of freeze-fractured intercellular junctions in the guinea pig inner ear. *Acta Otolaryngol.* **336**, 1-40.

Kikuchi, T., Kimura, R. S., Paul, D. L. and Adams, J. C. (1995). Gap junctions in the rat cochlea: immunohistochemical and ultrastructural analysis. *Anat. Embryol.* **191**, 101-118.

Kitajiri, S. I., Furuse, M., Morita, K., Saishin-Kiuchi, Y., Kido, H., Ito, J. and Tsukita, S. (2004). Expression patterns of claudins, tight junction adhesion molecules, in the inner ear. *Hear. Res.* **187**, 25-34.

Kiuchi-Saishin, Y., Gotoh, S., Furuse, M., Takasuga, A., Tano, Y. and Tsukita, S. (2002). Differential expression patterns of claudins, tight junction membrane proteins, in mouse nephron segments. *J. Am. Soc. Nephrol.* **13**, 875-886.

Konishi, T., Hamrick, P. E. and Walsh, P. J. (1978). Ion transport in guinea pig cochlea. I. Potassium and sodium transport. *Acta Otolaryngol.* **86**, 22-34.

Marcus, D. C., Wu, T., Wangemann, P. and Kofuji, P. (2002). KCNJ10 (Kir4.1) potassium channel knockout abolishes endocochlear potential. *Am. J. Physiol.* **282**, C403-C407.

Martin-Padura, I., Lostaglio, S., Schneemann, M., Williams, L., Romano, M., Fruscella, P., Panzeri, C., Stoppacciaro, A., Ruco, L., Villa, A. et al. (1998). Junctional adhesion molecule, a novel member of the immunoglobulin superfamily that distributes at intercellular junctions and modulates monocyte transmigration. *J. Cell Biol.* **142**, 117-127.

Mitic, L. L. and Anderson, J. M. (1998). Molecular architecture of tight junctions. *Annu. Rev. Physiol.* **60**, 121-142.

Morita, K., Furuse, M., Fujimoto, K. and Tsukita, S. (1999a). Claudin multigene family encoding four-transmembrane domain protein components of tight junction strands. *Proc. Natl. Acad. Sci. USA* **96**, 511-516.

Morita, K., Sasaki, H., Fujimoto, K., Furuse, M. and Tsukita, S. (1999b). Claudin-11/OSP-based tight junctions in myelinated sheaths of oligodendrocytes and Sertoli cells in testis. *J. Cell Biol.* **145**, 579-588.

Nitta, T., Hata, M., Gotoh, S., Seo, Y., Sasaki, H., Hashimoto, N., Furuse, M. and Tsukita, S. (2003). Size-selective loosening of the blood-brain barrier in claudin-5-deficient mice. *J. Cell Biol.* **161**, 653-660.

Offner, F. F., Dallos, P. and Cheatham, M. A. (1987). Positive endocochlear potential: mechanism of production by marginal cells of stria vascularis. *Hear. Res.* **29**, 117-124.

Russell, L. D. and Peterson, R. N. (1985). Sertoli cell junctions: morphological and functional correlates. *Int. Rev. Cytol.* **94**, 177-211.

Saitou, M., Ando-Akatsuka, Y., Itoh, M., Furuse, M., Inazawa, J., Fujimoto, K. and Tsukita, S.-H. (1997). Mammalian occludin in epithelial cells: its expression and subcellular distribution. *Eur. J. Cell Biol.* **73**, 222-231.

Salt, A. N., Melichar, I. and Thalmann, R. (1987). Mechanisms of endocochlear potential generation by stria vascularis. *Laryngoscope* **97**, 984-991.

Schneeberger, E. E. and Lynch, R. D. (1992). Structure, function, and regulation of cellular tight junctions. *Am. J. Physiol.* **262**, L647-L661.

Staehelin, L. A. (1974). Structure and function of intercellular junctions. *Int. Rev. Cytol.* **39**, 191-283.

Sterkers, O., Ferrary, E. and Amiel, C. (1988). Production of inner ear fluids. *Phys. Rev.* **68**, 1083-1128.

Takamaki, A., Mori, Y., Araki, M., Mineharu, A., Sohma, Y., Tashiro, J., Yoshida, R., Takenaka, H. and Kubota, T. (2003). Asphyxia and diuretic-induced changes in the Ca^{2+} concentration of endolymph. *Jpn J. Physiol.* **53**, 35-44.

Takeuchi, S., Ando, M., Kozakura, K., Saito, H. and Irimajiri, A. (1995). Ion channels in basolateral membrane of marginal cells dissociated from gerbil stria vascularis. *Hear. Res.* **83**, 89-100.

Takeuchi, S., Ando, M. and Kakigi, A. (2000). Mechanism generating endocochlear potential: role played by intermediate cells in stria vascularis. *Biophys. J.* **79**, 2572-2582.

Tasaki, I. and Spyroupoulos, C. S. (1959). Stria vascularis as source of endocochlear potential. *J. Neurophysiol.* **22**, 149-155.

Tsukita, S.-H. and Furuse, M. (1999). Occludin and claudins in tight junction strands: leading or supporting players? *Trends Cell Biol.* **9**, 268-273.

Tsukita, S.-H., Furuse, M. and Itoh, M. (2001). Multifunctional strands in tight junctions. *Nat. Rev. Mol. Cell Biol.* **2**, 285-293.

von Bekesy, G. (1950). DC potentials and energy balance of the cochlear partition. *J. Acoust. Soc. Am.* **22**, 576-582.

Wangemann, P. (1995). Comparison of ion transport mechanisms between vestibular dark cells and strial marginal cells. *Hear. Res.* **90**, 149-157.

Wangemann, P. (2002). K^+ cycling and the endocochlear potential. *Hear. Res.* **165**, 1-9.

Wangemann, P. and Schacht, J. (1996). Homeostasic mechanisms in the cochlea. In *Springer Handbook of Auditory Research: The Cochlea* (eds P. Dallos, A. N. Popper and R. Fay), pp. 130-185. Berlin, Germany: Springer.

Wangemann, P., Liu, J. and Marcus, D. C. (1995). Ion transport mechanisms responsible for K^+ secretion and the transepithelial voltage across marginal cells of stria vascularis in vitro. *Hear. Res.* **84**, 19-29.

Wilcox, E. R., Burton, Q. L., Naz, S., Riazuddin, S., Smith, T. N., Ploplis, B., Belyantseva, I., Ben-Yosef, T., Liburd, N. A., Morell, R. J. et al. (2001). Mutations in the gene encoding tight junction claudin-14 cause autosomal recessive deafness DFNB29. *Cell* **104**, 165-172.

Zheng, Q. Y., Johnson, K. R. and Erway, L. C. (1999). Assessment of hearing in 80 inbred strains of mice by ABR threshold analyses. *Hear. Res.* **13**, 94-107.